Supplementary Figures

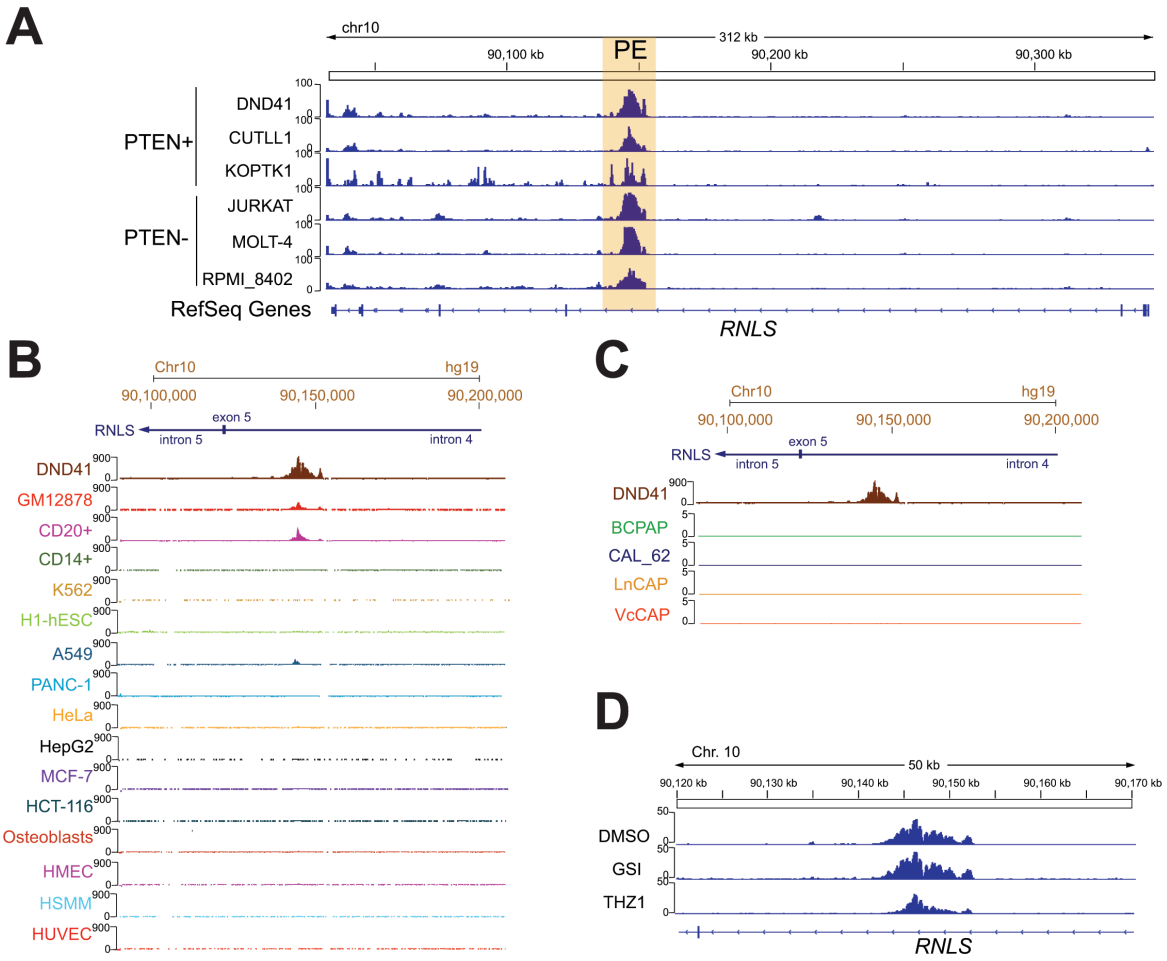

Supplementary Figure 1. H3K27ac ChIP-seq and Hi-C analyses along the human PE sequence. **A,** H3K27ac mark along the PE sequence in both PTEN-positive and PTEN-negative T-ALL cell lines. **B,** H3K27ac mark along the PE sequence in cells and cell lines from ENCODE, including DND41 T-ALL cells, GM12878 lymphoblastoid cells, B cells (CD20+), monocytes (CD14+), K562 erythroleukemia cells, H1 human embryonic stem cells, H1-hESC), A549 lung cancer cells, PANC-1 pancreatic cancer cells, HeLa cervical cancer cells, HepG2 liver cancer cells, MCF-7 breast cancer cells, HCT-116 colon cancer cells, osteoblasts, human mammary epithelial cells (HMEC), human skeletal muscle myoblast cells (HSMM) and human umbilical vein endothelial cells (HUVEC). **C,** H3K27ac mark along the PE sequence in DND41 T-ALL cells, as well as in BCPAP or CAL_62 thyroid cancer cells (24) and LnCAP or VcCAP prostate cancer cells (23). **D,** H3K27ac mark along the PE sequence in CUTLL1 control cells (DMSO), treated with a GSI or with a CDK7 inhibitor (THZ1) (19). **E-F**, Hi-C interaction profile (19) of the *PTEN* promoter and the PE enhancer in CD4 control T-cells (**E**) and a human primary T-ALL sample (**F**). Interaction is highlighted by black circles. RefSeq genes and H3K27ac mark in DND41 cells are shown as reference.

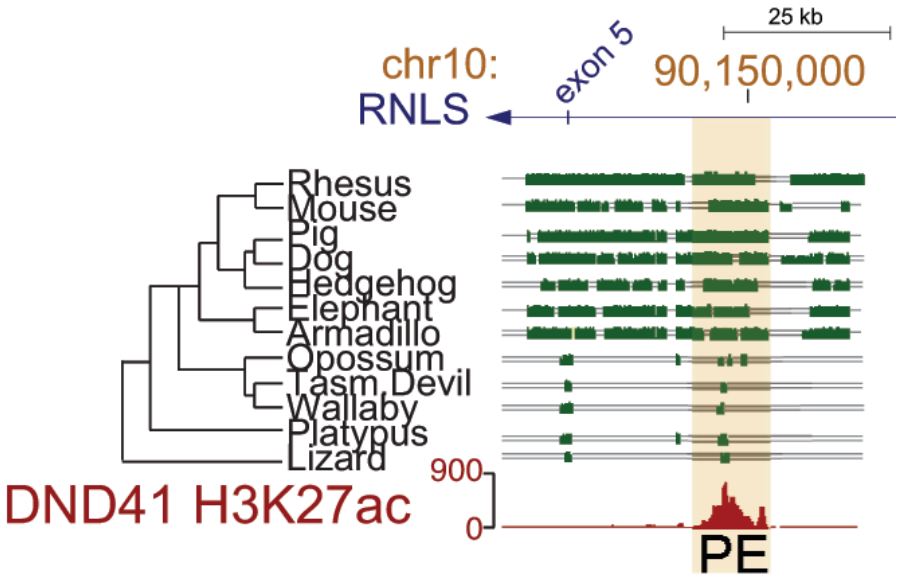

Supplementary Figure 2. Conservation of the PE DNA sequence. Multispecies sequence conservation along a 50Kb window encompassing the DND41 H3K27 acetylation mark in PE (bottom). Green blocks represent pairwise aligned regions, and the height of the bars indicates the average base pair alignment score with the human sequence

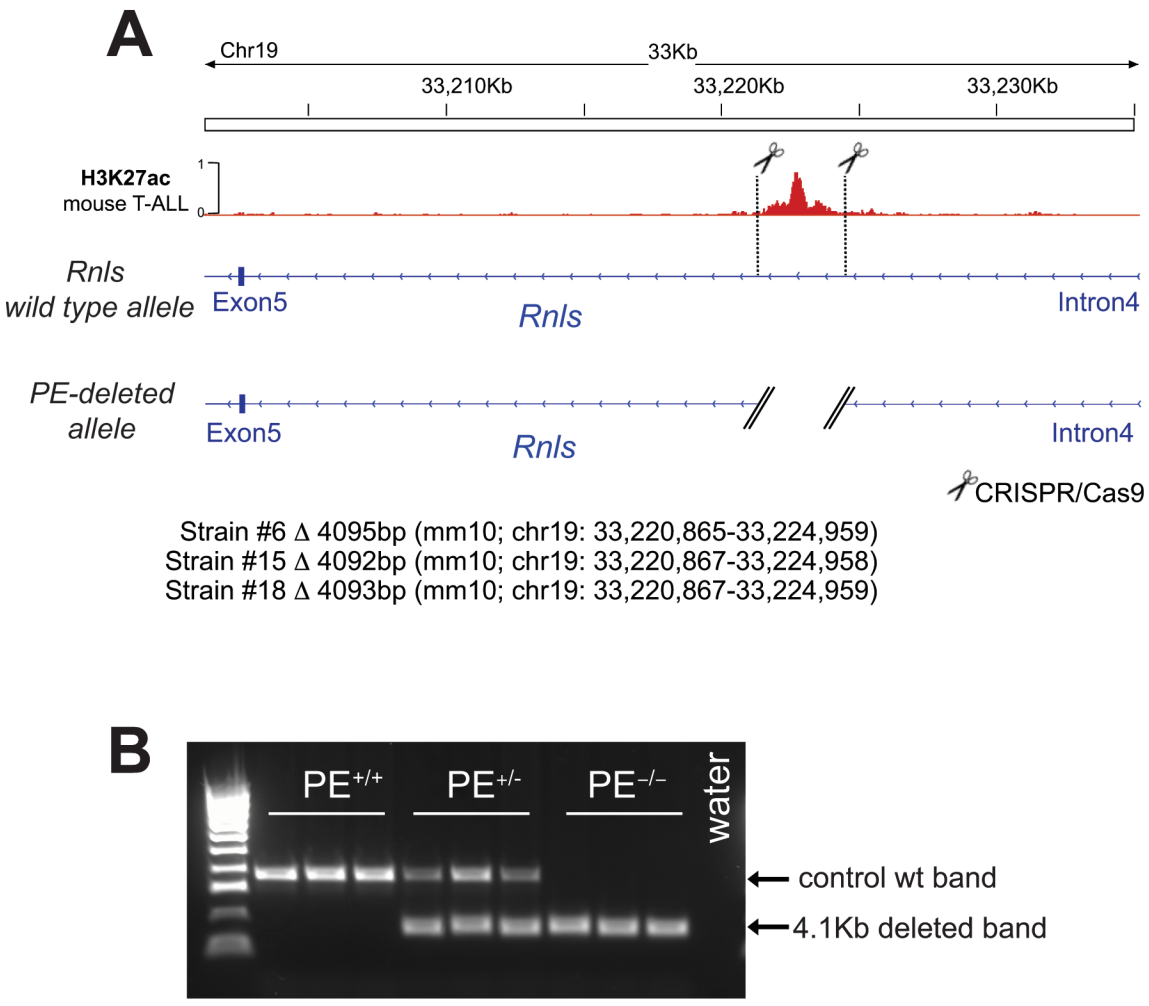

Supplementary Figure 3. Generation of novel mouse models with PE germinal deletion. **A,** Schematic representation of the wild type *Rnls* locus and CRISPR/Cas9-strategy to obtain PE knockout mice. Strain-specific deletion coordinates are shown at the bottom. **B,** Genotyping of PE knockout mice.

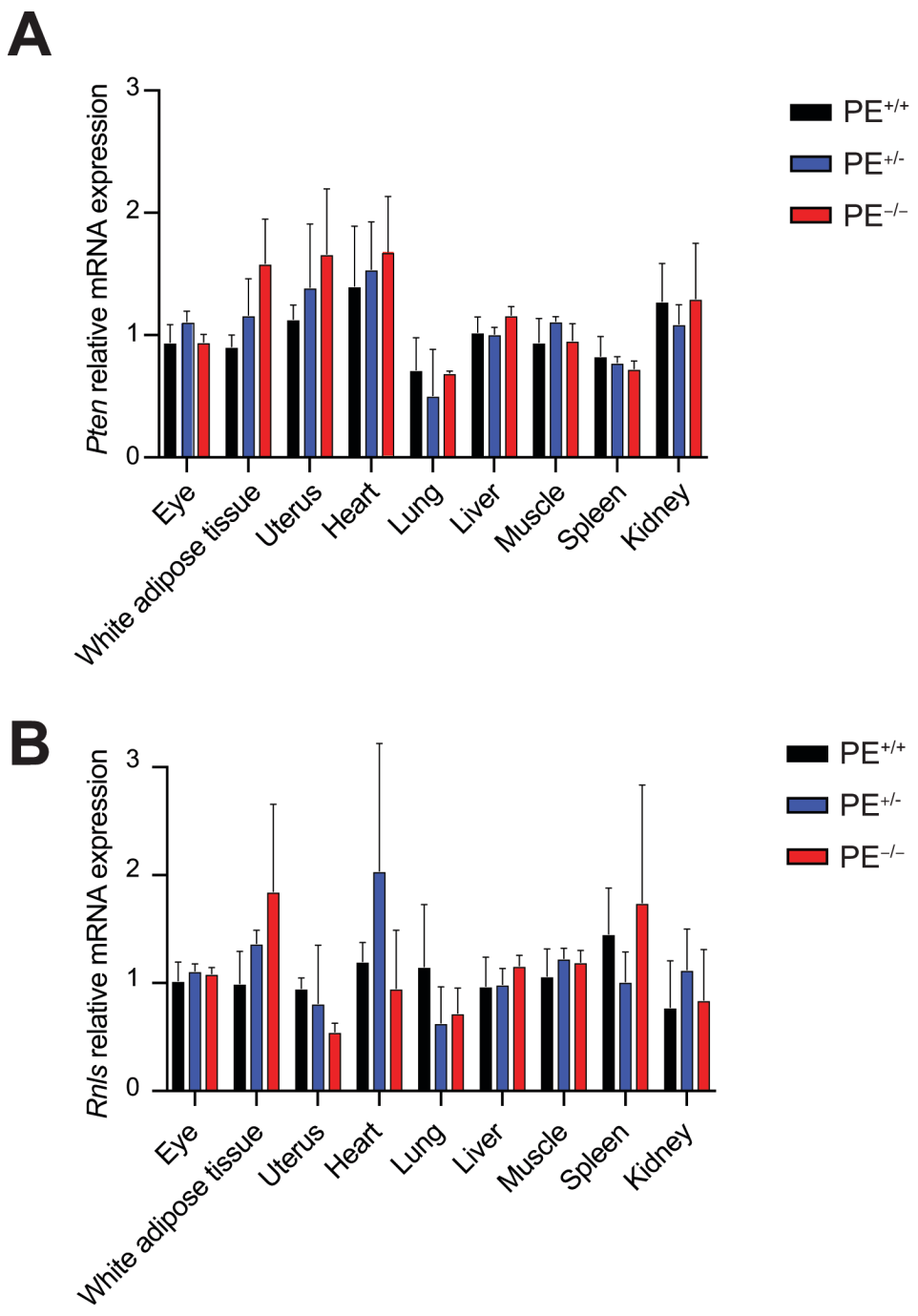

Supplementary Figure 4. *Pten* and *Rnls* expression in non-thymic tissues. **A-B,** RT-PCR analysis of *Pten* expression (**A**) and *Rnls* expression (**B**) in tissues obtained from PE wild-type and PE heterozygous or PE knockout mice. Bar graphs indicate mean values and error bars represent s.d.

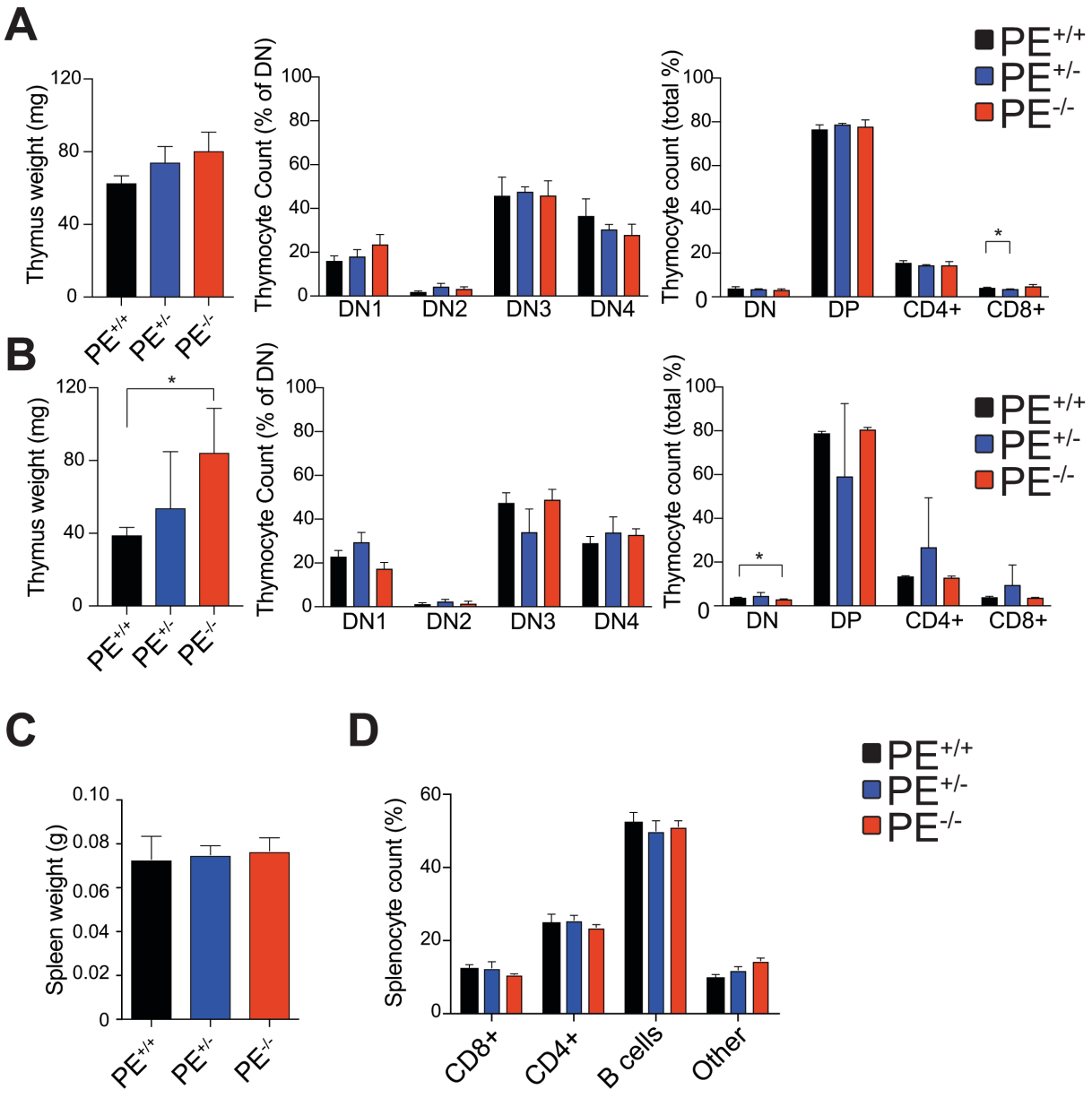

Supplementary Figure 5. Immunophenotypic analyses of PE wild-type, heterozygous or knockout mice. **A-B,** Thymus weight and quantification of intrathymic T-cell populations in 6-week-old wild-type ($PE^{+/+}$), PE heterozygous knockout ($PE^{+/-}$) and PE homozygous knockout ($PE^{-/-}$) mice from strain #15 (**A**) or strain #18 (**B**) (n = 3 per genotype). **C-D,** Spleen weight (**C**) and quantification of lymphoid populations (**D**) in 6-week-old wild-type ($PE^{+/+}$), PE heterozygous knockout ($PE^{+/-}$) and PE homozygous knockout ($PE^{-/-}$) mice

45 (strain #6; n = 3 per genotype). Bar graphs indicate mean values and error bars represent
46 s.d. Significance was calculated using two-tailed Student's t- test (*P < 0.05; all other
47 comparisons not significant).
48

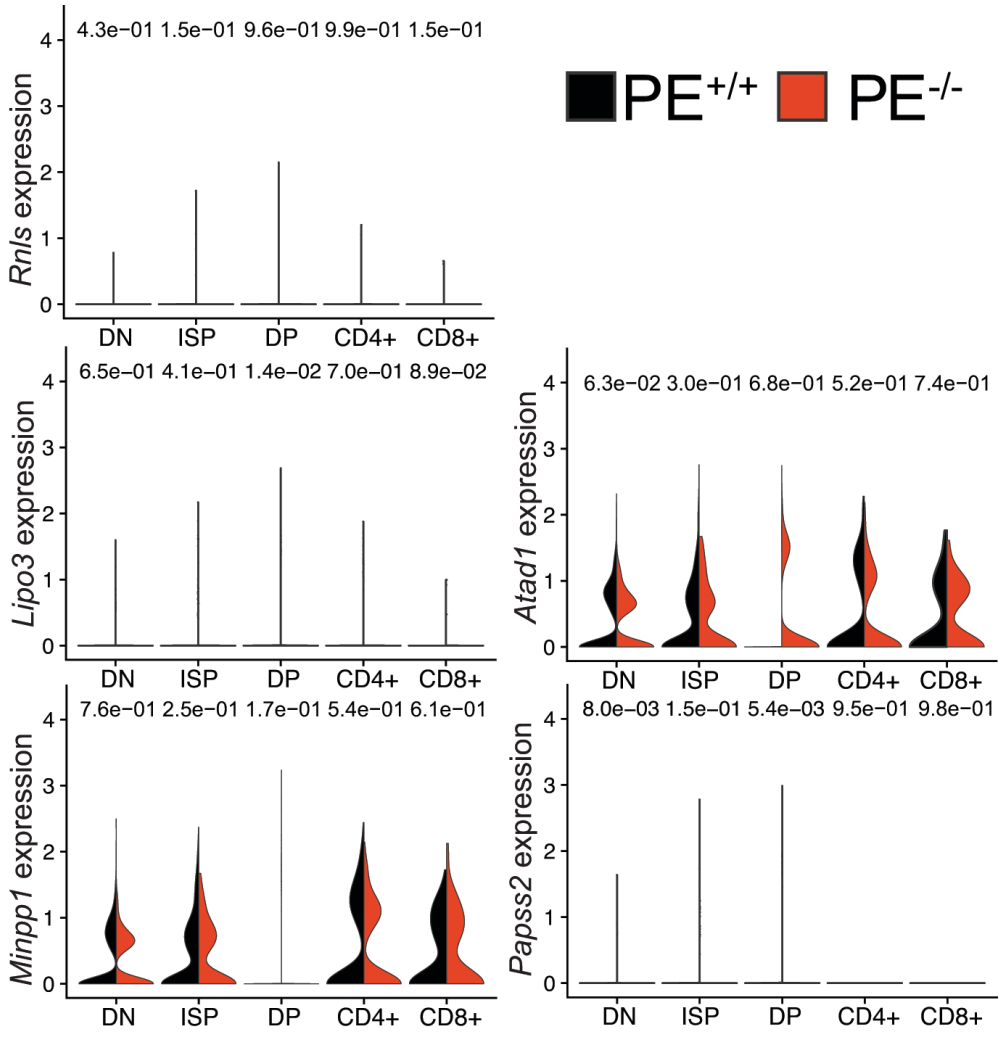

Supplementary Figure 6. Gene expression changes upon PE loss. Gene expression changes in *Rnls* and other genes in neighboring TADs (*Atad1*, *Minpp1*, *Lipo3*, *Papss2*) in scRNA-seq from normal thymus. *P* values in A calculated using the Wilcoxon rank-sum test (no significant values were found).

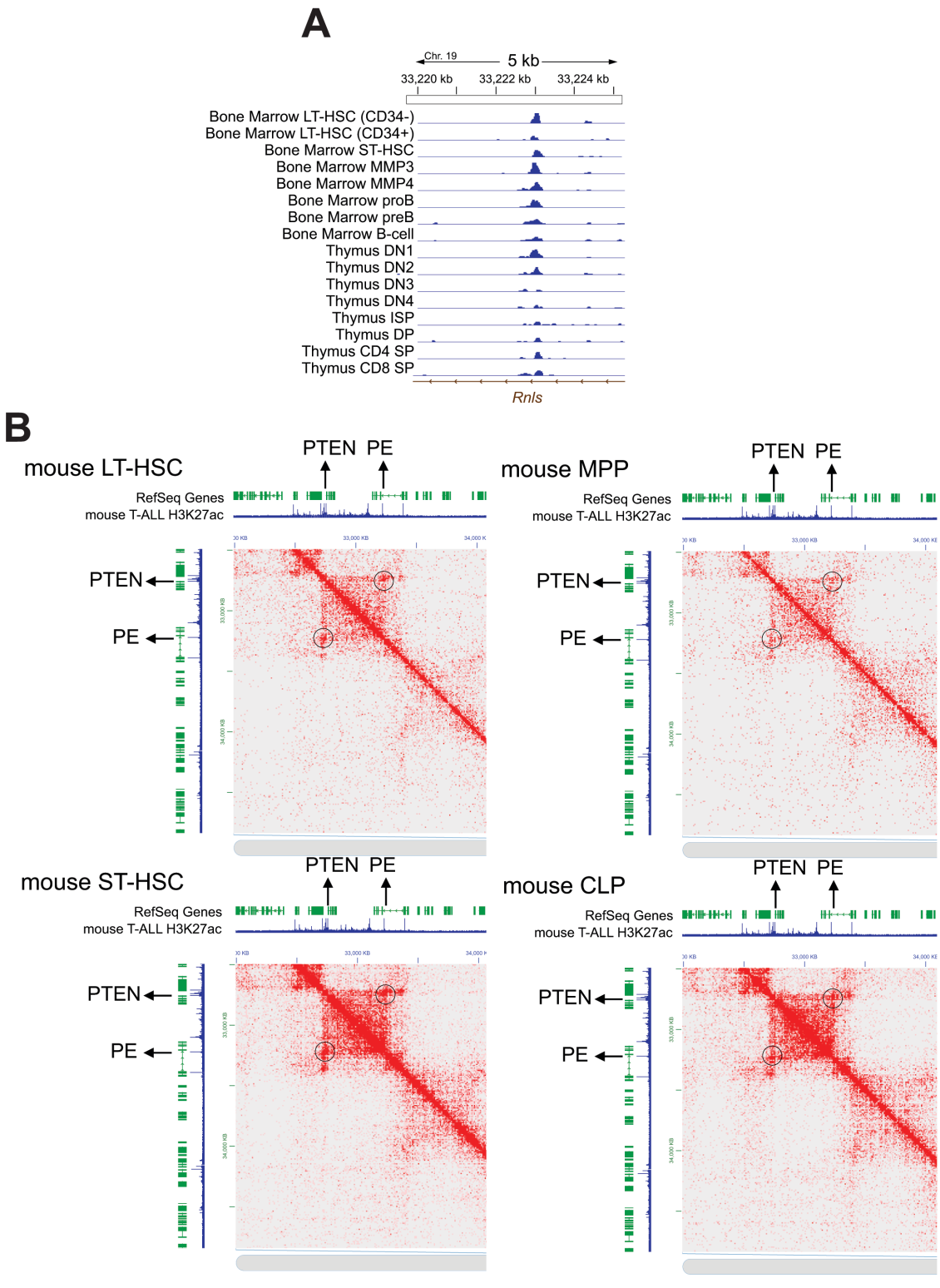
A
Chr. 19
5 kb
33,220 kb
33,222 kb
33,224 kb
Bone Marrow LT-HSC (CD34-)
Bone Marrow LT-HSC (CD34+)
Bone Marrow ST-HSC
Bone Marrow MMP3
Bone Marrow MMP4
Bone Marrow proB
Bone Marrow preB
Bone Marrow B-cell
Thymus DN1
Thymus DN2
Thymus DN3
Thymus DN4
Thymus ISP
Thymus DP
Thymus CD4 SP
Thymus CD8 SP
Rnls
B
mouse LT-HSC
PTEN PE
RefSeq Genes
mouse T-ALL H3K27ac
PTEN
PE
mouse MPP
PTEN PE
RefSeq Genes
mouse T-ALL H3K27ac
PTEN
PE
mouse ST-HSC
PTEN PE
RefSeq Genes
mouse T-ALL H3K27ac
PTEN
PE
mouse CLP
PTEN PE
RefSeq Genes
mouse T-ALL H3K27ac
PTEN
PE

Supplementary Figure 7. ATAC-seq and tagHi-C analyses along the mouse PE sequence. **A,** ATACseq (GSE100738) showing open chromatin in PE in different mouse hematopoietic populations (LT-HSC= Long-Term Hematopoietic Stem Cells; ST-HSC= Short-Term Hematopoietic Stem Cells; MMP=Multipotent Progenitors; DN= CD4/CD8-Double Negative; ISP=Immature Single Positive; DP= CD4/CD8-Double Positive; SP= Single Positive). **B,** tagHi-C interactions (GSE152918) between the *Pten* promoter and the PE enhancer in different mouse hematopoietic progenitor cells. Interaction is highlighted by black circles. RefSeq genes and H3K27ac mark in mouse T-ALL cells are shown as reference.

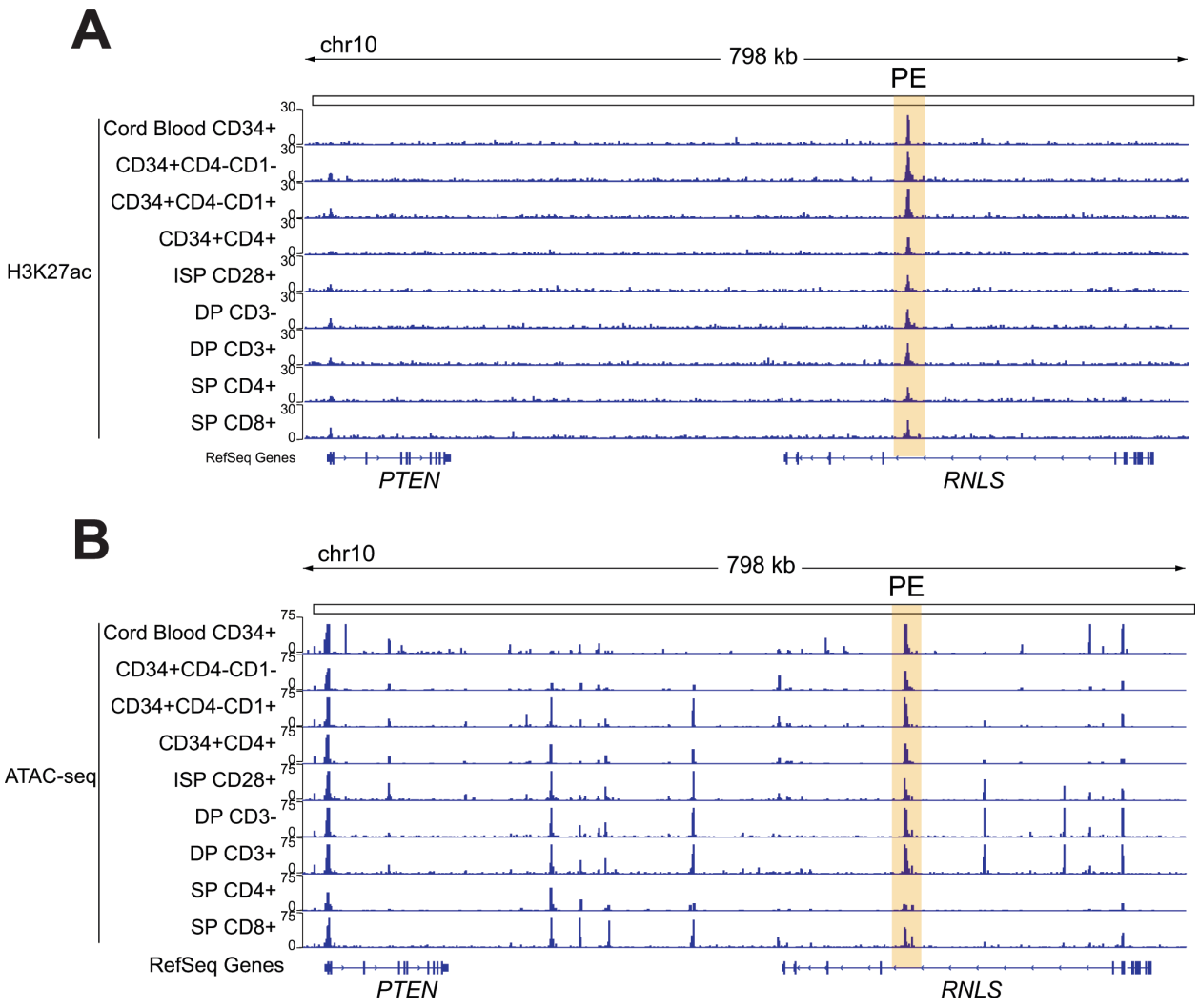

Supplementary Figure 8. Chromatin marks and chromatin opening in different human hematopoietic and thymic populations. H3K27ac ChIPmentation tracks (**A**) and ATAC-seq tracks (**B**) in human hematopoietic and thymic populations (ISP=Immature Single Positive; DP= CD4/CD8-double positive; SP= Single Positive).

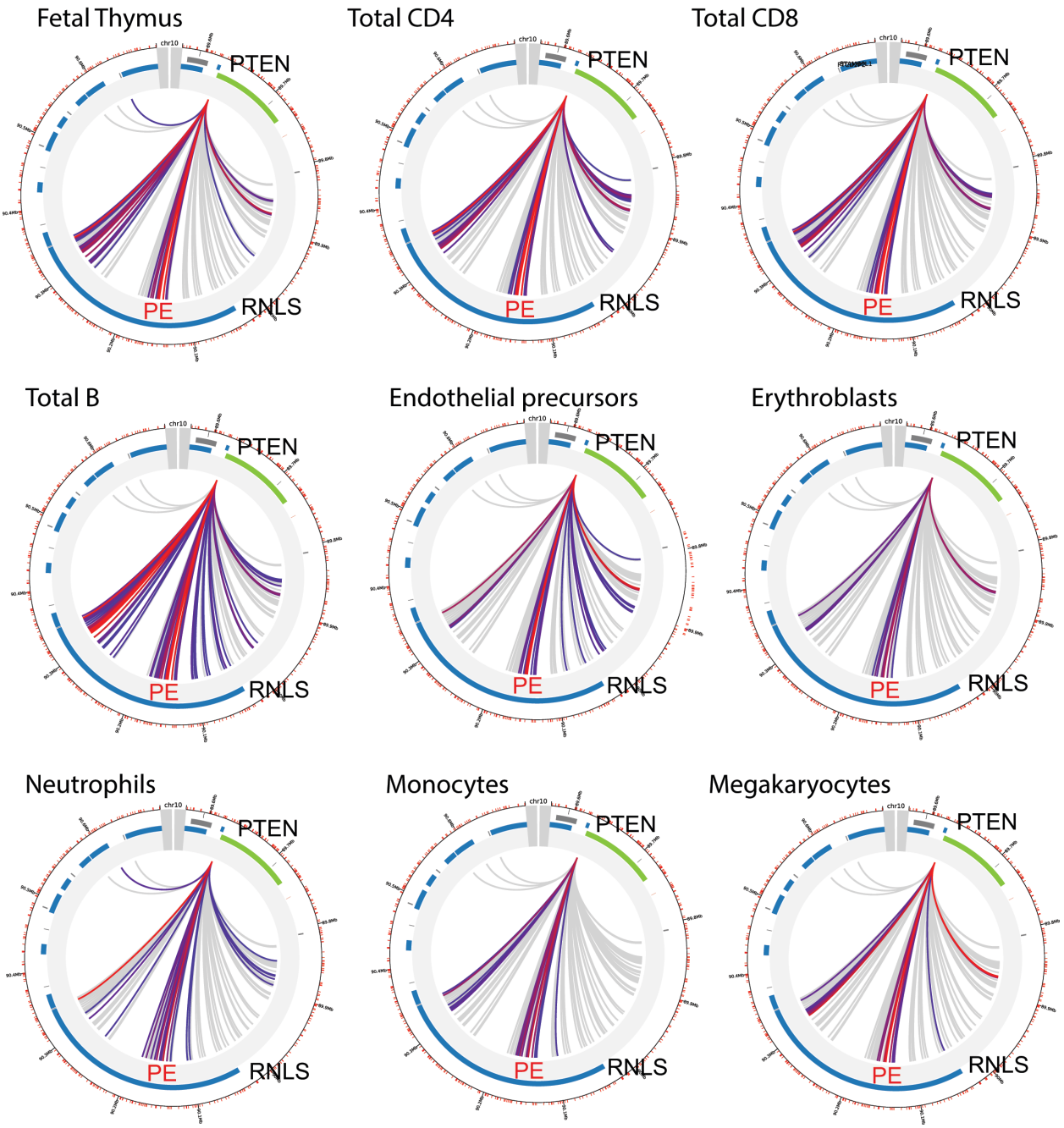

Supplementary Figure 9. Capture Hi-C shows interaction between the *PTEN* promoter and the PE enhancer in different human hematopoietic cells. Red/blue/gray lines represent interaction scores (70) (red=strongest; gray=weakest). PE is highlighted in red.

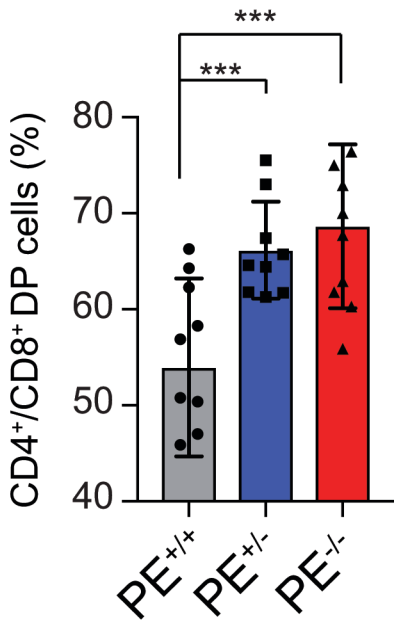

Supplementary Figure 10. CD4/CD8-double positive cells in peripheral blood 3 weeks after transplantation of NOTCH1-infected bone marrow progenitor cells (strain#6). ***$P <$ 0.005 using two-tailed Student's *t*-test.

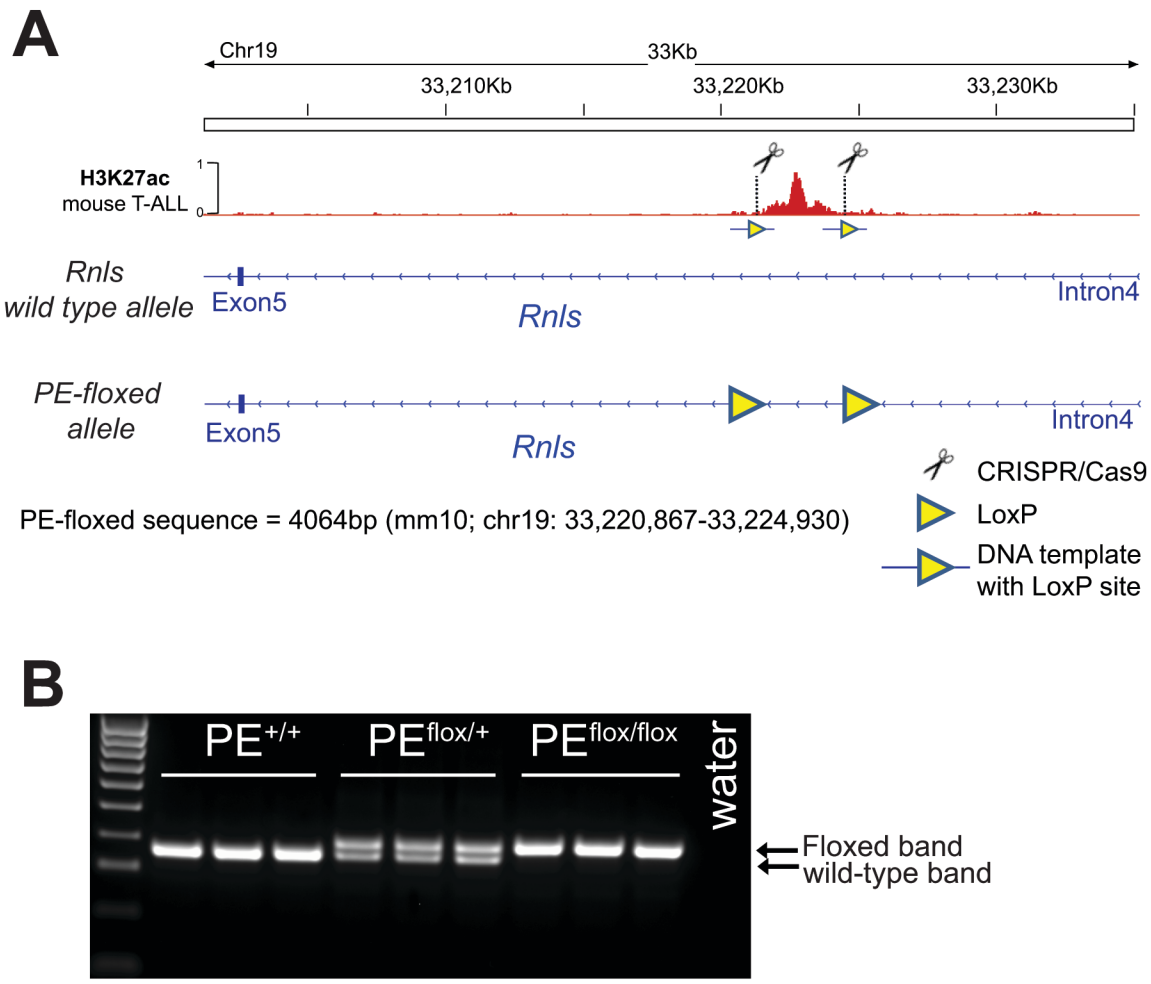

83

84 **Supplementary Figure 11.** Generation of PE conditional knockout mice. **A,** Schematic

85 representation of the wild type *Rnls* locus and CRISPR/Cas9-strategy to obtain PE

86 knockout mice. Specific coordinates of the floxed region are shown at the bottom. **B,**

87 Genotyping of PE conditional knockout mice.

88

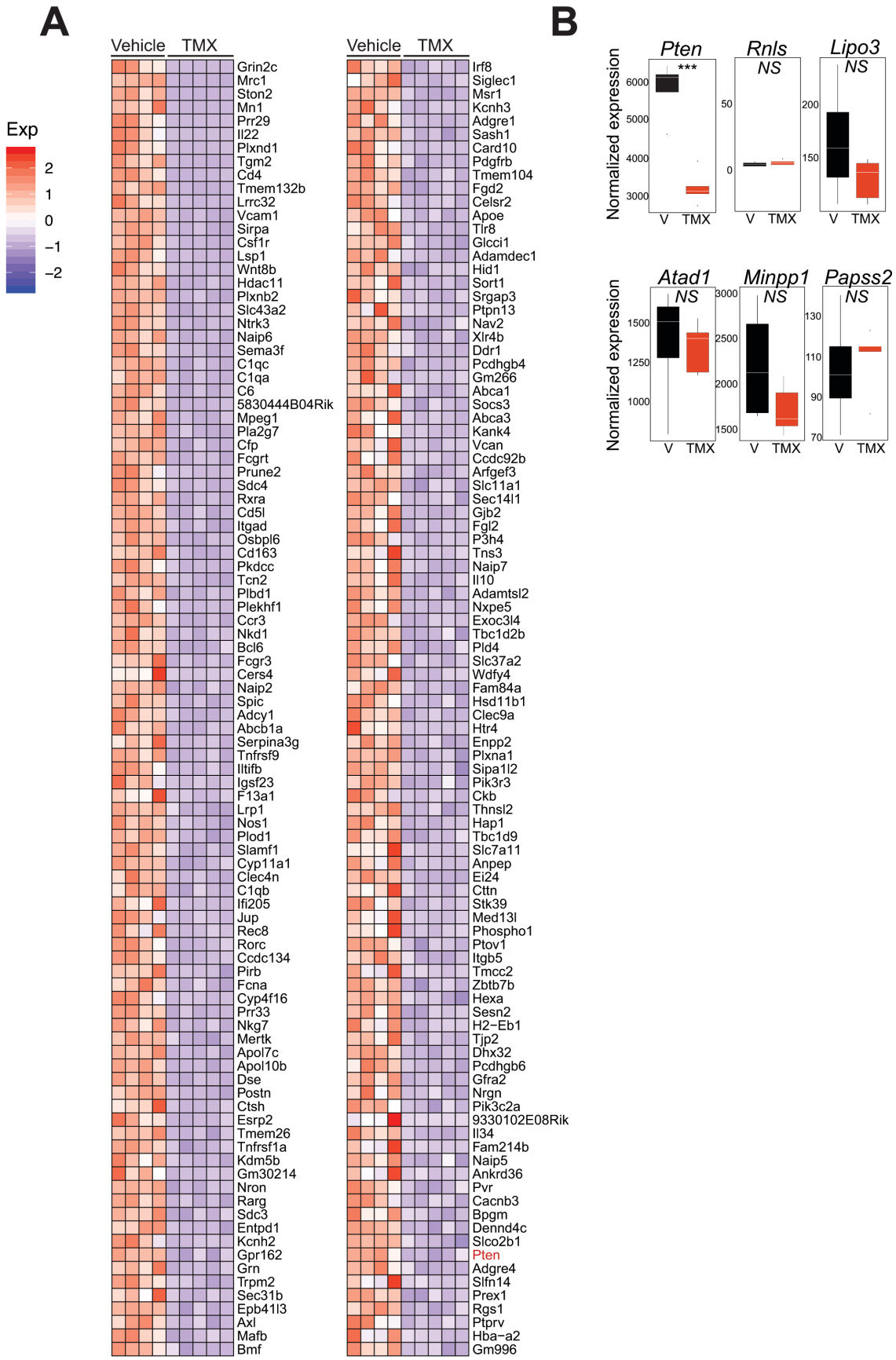
A
Vehicle
TMX
Exp
2
1
0
−1
−2
Grin2c
Mrc1
Ston2
Mn1
Prr29
Il22
Plxnd1
Tgm2
Cd4
Tmem132b
Lrrc32
Vcam1
Sirpa
Csf1r
Lsp1
Wnt8b
Hdac11
Plxnb2
Slc43a2
Ntrk3
Naip6
Sema3f
C1qc
C1qa
C6
5830444B04Rik
Mpeg1
Pla2g7
Cfp
Fcgrt
Prune2
Sdc4
Rxra
Cd5l
Itgad
Osbpl6
Cd163
Pkdcc
Tcn2
Plbd1
Plekhf1
Ccr3
Nkd1
Bcl6
Fcgr3
Cers4
Naip2
Spic
Adcy1
Abcb1a
Serpina3g
Tnfrsf9
Iltifb
Igsf23
F13a1
Lrp1
Nos1
Plod1
Slamf1
Cyp11a1
Clec4n
C1qb
Ifi205
Jup
Rec8
Rorc
Ccdc134
Pirb
Fcna
Cyp4f16
Prr33
Nkg7
Mertk
Apol7c
Apol10b
Dse
Postn
Ctsh
Esrp2
Tmem26
Tnfrsf1a
Kdm5b
Gm30214
Nron
Rarg
Sdc3
Entpd1
Kcnh2
Gpr162
Grn
Trpm2
Sec31b
Epb41l3
Axl
Mafb
Bmf
Vehicle
TMX
Irf8
Siglec1
Msr1
Kcnh3
Adgre1
Sash1
Card10
Pdgfrb
Tmem104
Fgd2
Celsr2
Apoe
Tlr8
Glcci1
Adamdec1
Hid1
Sort1
Srgap3
Ptpn13
Nav2
Xlr4b
Ddr1
Pcdhgb4
Gm266
Abca1
Socs3
Abca3
Kank4
Vcan
Ccdc92b
Arfgef3
Slc11a1
Sec14l1
Gjb2
Fgl2
P3h4
Tns3
Naip7
Il10
Adamtsl2
Nxpe5
Exoc3l4
Tbc1d2b
Pld4
Slc37a2
Wdfy4
Fam84a
Hsd11b1
Clec9a
Htr4
Enpp2
Plxna1
Sipa1l2
Pik3r3
Ckb
Thnsl2
Hap1
Tbc1d9
Slc7a11
Anpep
Ei24
Cttn
Stk39
Med13l
Phospho1
Ptov1
Itgb5
Tmcc2
Zbtb7b
Hexa
Sesn2
H2−Eb1
Tjp2
Dhx32
Pcdhgb6
Gfra2
Nrgn
Pik3c2a
9330102E08Rik
Il34
Fam214b
Naip5
Ankrd36
Pvr
Cacnb3
Bpgm
Dennd4c
Slco2b1
Pten
Adgre4
Slfn14
Prex1
Rgs1
Ptprv
Hba−a2
Gm996
B
Pten
***
Rnls
NS
Lipo3
NS
Normalized expression
6000
5000
4000
3000
50
0
200
150
V
TMX
Atad1
NS
Minpp1
NS
Papss2
NS
1500
1250
1000
3000
2500
2000
1500
130
110
90
70

Supplementary Figure 12. Gene expression changes upon secondary loss of PE in mouse T-ALL. **A,** Full heat map list of downregulated genes upon secondary PE loss in PE conditional knockout T-ALL. Cutoffs used: Wald statistic < -5 or > 5; *P*-adjusted value < 1E-04). **B,** Gene expression changes in *Pten*, *Rnls* and other genes in neighboring TADs (*Atad1*, *Minpp1*, *Lipo3*, *Papss2*) treated with Vehicle (V) or Tamoxifen (TMX) to induce PE loss. Significance calculated using the Mann-Whitney test (****P* <1E-04; NS=not significant).

A

SAMPLE NAME	*PTEN* CDS deletions	PE enhancer deletions	*NOTCH1*/*FBXW7* mutational status
SJALL015247_D1-PARMIH	89623758-89690024 (heterozygous) 89690024-89932052 (homozygous)	89932052-90171290 (heterozygous)	MUTANT
SJALL015278_D1-PARJPL	89251655-89629121 (heterozygous) 89629531-89779737 (homozygous)	89952294-90165341 (homozygous)	MUTANT
SJALL015688_D1-PATSIL	89081178-89626462 (heterozygous) 89626462-89663879 (heterozygous) 89663879-89702405 (heterozygous) 89702405-89745782 (heterozygous)	89745782-90940820 (heterozygous)	MUTANT
SJALL002373_D1-PASKCL	WT	89755359-91198159 (heterozygous)	WT
SJALL0085_D	89613581-89636910 (heterozygous) 89636910-89642937 (heterozygous) 89642937-89755359 (heterozygous)	89755359-90787680 (homozygous)	WT

B Normal donor T-cells

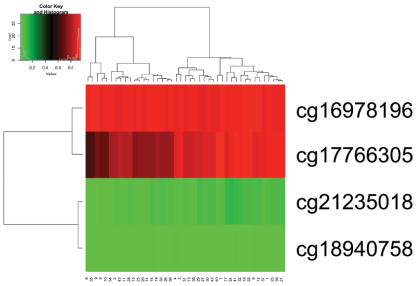

C T-ALL Sanger Cell lines

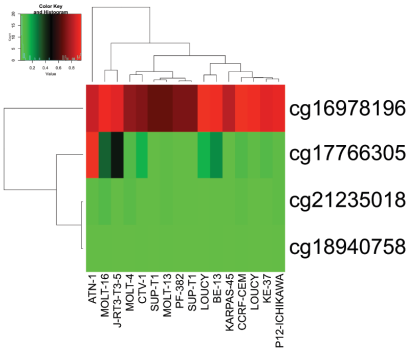

D T-ALL primary samples

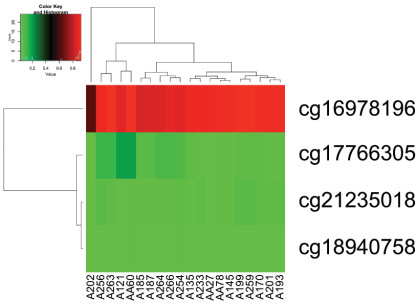

Supplementary Figure 13. Genomic deletions and DNA methylation along the PE sequence in human T-ALL primary samples. **A,** Table showings specific genomic coordinates of deletions in *PTEN* and/or PE, as well as NOTCH1/FBXW7 mutational status in human primary T-ALL samples. **B-D,** Unsupervised clustering (euclidean distance, complete-linkage clustering) and heatmap of the 4 CpGs sites in the PE sequence in healthy donors T-cells (**B**), human T-ALL cell lines (**C**) or human T-ALL primary samples (**D**). Green and red colors represent methylation Beta values: green for hypomethylation and red for hypermethylation. CpGs are displayed in rows and samples in columns.

Strain 6 $PE^{+/-}$ x $PE^{+/-}$		
Genotype	Expected Mendelian genetic frequencies (%)	Observed frequencies (%) (n=364)
$PE^{+/+}$	25 (50% females, 50% males)	25 (54% females, 46% males)
$PE^{+/-}$	50 (50% females, 50% males)	53 (53% females, 47% males)
$PE^{-/-}$	25 (50% females, 50% males)	22 (54% females, 46% males)

Strain 15 $PE^{+/-}$ x $PE^{+/-}$		
Genotype	Expected Mendelian genetic frequencies (%)	Observed frequencies (%) (n=192)
$PE^{+/+}$	25 (50% females, 50% males)	25.5 (55% females, 45% males)
$PE^{+/-}$	50 (50% females, 50% males)	46 (44% females, 56% males)
$PE^{-/-}$	25 (50% females, 50% males)	28.5 (42% females, 58% males)

Strain 18 $PE^{+/-}$ x $PE^{+/-}$		
Genotype	Expected Mendelian genetic frequencies (%)	Observed frequencies (%) (n=342)
$PE^{+/+}$	25 (50% females, 50% males)	23 (45% females, 45% males)
$PE^{+/-}$	50 (50% females, 50% males)	53 (52% females, 48% males)
$PE^{-/-}$	25 (50% females, 50% males)	24 (59% females, 41% males)

Supplementary Table 1. Genetic frequencies in $PE^{+/-}$ x $PE^{+/-}$ offsprings.

NAME	NOM p-val
KEGG_PRION_DISEASES	0
APPEL_IMATINIB_RESPONSE	0
ICHIBA_GRAFT_VERSUS_HOST_DISEASE_35D_UP	0
LEE_AGING_CEREBELLUM_UP	0
LIAN_LIPA_TARGETS_6M	0
BOQUEST_STEM_CELL_CULTURED_VS_FRESH_DN	0
LIAN_LIPA_TARGETS_3M	0
ICHIBA_GRAFT_VERSUS_HOST_DISEASE_D7_UP	0
VALK_AML_CLUSTER_5	0
PAL_PRMT5_TARGETS_DN	0
ROSS_AML_WITH_CBFB_MYH11_FUSION	0
NADLER_OBESITY_UP	0
MARKEY_RB1_CHRONIC_LOF_DN	0
DACOSTA_ERCC3_ALLELE_XPCS_VS_TTD_UP	0
YAMASHITA_LIVER_CANCER_STEM_CELL_UP	0
STEARMAN_TUMOR_FIELD_EFFECT_UP	0
MOREAUX_B_LYMPHOCYTE_MATURATION_BY_TACI_UP	0
KEGG_TOLL_LIKE_RECEPTOR_SIGNALING_PATHWAY	0
COATES_MACROPHAGE_M1_VS_M2_UP	0
KEGG_LYSOSOME	0
RAMALHO_STEMNESS_DN	0
PAPASPYRIDONOS_UNSTABLE_ATEROSCLEROTIC_PLAQUE_UP	0
RUTELLA_RESPONSE_TO_CSF2RB_AND_IL4_DN	0
KEGG_THYROID_CANCER	0
LENAOUR_DENDRITIC_CELL_MATURATION_UP	0
DORSAM_HOXA9_TARGETS_DN	0
LEE_LIVER_CANCER_CIPROFIBRATE_UP	0
WILENSKY_RESPONSE_TO_DARAPLADIB	0
KEGG_ABC_TRANSPORTERS	0
GAL_LEUKEMIC_STEM_CELL_UP	0
RUTELLA_RESPONSE_TO_HGF_VS_CSF2RB_AND_IL4_UP	0
HOSHIDA_LIVER_CANCER_LATE_RECURRENCE_UP	0
ZHAN_MULTIPLE_MYELOMA_DN	0
RADMACHER_AML_PROGNOSIS	0
RUTELLA_RESPONSE_TO_HGF_UP	0
LIU_VAV3_PROSTATE_CARCINOGENESIS_UP	0
STEARMAN_LUNG_CANCER_EARLY_VS_LATE_DN	0
REACTOME_DISEASES_OF_IMMUNE_SYSTEM	0
NAKAMURA_CANCER_MICROENVIRONMENT_UP	0
OZANNE_AP1_TARGETS_UP	0
MCBRYAN_PUBERTAL_BREAST_5_6WK_DN	0
KUROZUMI_RESPONSE_TO_ONCOCYTIC_VIRUS_AND_CYCLIC_RGD	0
KATSANOU_ELAVL1_TARGETS_UP	0
KYNG_WERNER_SYNDROM_DN	0

PID_INTEGRIN2_PATHWAY	0
PID_ANTHRAX_PATHWAY	0
REACTOME_TRANSCRIPTIONAL_REGULATION_OF_WHITE_ADIPOC	0
SHIN_B_CELL_LYMPHOMA_CLUSTER_3	0
REACTOME_NUCLEOBASE_CATABOLISM	0
JAATINEN_HEMATOPOIETIC_STEM_CELL_DN	0
ADDYA_ERYTHROID_DIFFERENTIATION_BY_HEMIN	0
BROWNE_HCMV_INFECTION_2HR_UP	0
REACTOME_NUCLEAR_RECEPTOR_TRANSCRIPTION_PATHWAY	0
PID_RETINOIC_ACID_PATHWAY	0
PEPPER_CHRONIC_LYMPHOCYTIC_LEUKEMIA_UP	0
REACTOME_ROLE_OF_PHOSPHOLIPIDS_IN_PHAGOCYTOSIS	0
BASSO_HAIRY_CELL_LEUKEMIA_UP	0
FULCHER_INFLAMMATORY_RESPONSE_LECTIN_VS_LPS_DN	0
MARKEY_RB1_ACUTE_LOF_DN	0
REACTOME_OTHER_SEMAPHORIN_INTERACTIONS	0
SEKI_INFLAMMATORY_RESPONSE_LPS_DN	0
BROWN_MYELOID_CELL_DEVELOPMENT_UP	0
MCLACHLAN_DENTAL_CARIES_UP	0
GAUSSMANN_MLL_AF4_FUSION_TARGETS_D_UP	0
PETROVA_ENDOTHELIUM_LYMPHATIC_VS_BLOOD_DN	0
KEGG_LEISHMANIA_INFECTION	0
ZHAN_MULTIPLE_MYELOMA_CD1_UP	0
JAZAERI_BREAST_CANCER_BRCA1_VS_BRCA2_DN	0
RAMASWAMY_METASTASIS_DN	0
REACTOME_DISEASES_OF_GLYCOSYLATION	0
ODONNELL_TARGETS_OF_MYC_AND_TFRC_UP	0
ONDER_CDH1_TARGETS_1_UP	0
NAKAYAMA_SOFT_TISSUE_TUMORS_PCA1_UP	0
PID_IL23_PATHWAY	0
BIOCARTA_P53HYPOXIA_PATHWAY	0
PID_P38_ALPHA_BETA_DOWNSTREAM_PATHWAY	0
CHIN_BREAST_CANCER_COPY_NUMBER_UP	0
FISCHER_DIRECT_P53_TARGETS_META_ANALYSIS	0
REACTOME_ABC_TRANSPORTERS_IN_LIPID_HOMEOSTASIS	0
THUM_SYSTOLIC_HEART_FAILURE_UP	0
LINDSTEDT_DENDRITIC_CELL_MATURATION_D	0
REACTOME_GOLGI_ASSOCIATED_VESICLE_BIOGENESIS	0
RUTELLA_RESPONSE_TO_CSF2RB_AND_IL4_UP	0
LENAOUR_DENDRITIC_CELL_MATURATION_DN	0
QI_PLASMACYTOMA_UP	0
PID_INTEGRIN_A9B1_PATHWAY	0
ABBUD_LIF_SIGNALING_1_DN	0
WANG_BARRETTS_ESOPHAGUS_AND_ESOPHAGUS_CANCER_DN	0
MCBRYAN_PUBERTAL_TGFB1_TARGETS_UP	0

BOHN_PRIMARY_IMMUNODEFICIENCY_SYNDROM_DN	0
SANSOM_APC_TARGETS_DN	0
GOZGIT_ESR1_TARGETS_UP	0
WOOD_EBV_EBNA1_TARGETS_DN	0
MORI_EMU_MYC_LYMPHOMA_BY_ONSET_TIME_DN	0
WEIGEL_OXIDATIVE_STRESS_BY_HNE_AND_TBH	0
SMIRNOV_CIRCULATING_ENDOTHELIOCYTES_IN_CANCER_UP	0
DELYS_THYROID_CANCER_UP	0
REACTOME_INTERLEUKIN_4_AND_INTERLEUKIN_13_SIGNALING	0
REACTOME_TOLL_LIKE_RECEPTOR_CASCADES	0
TONKS_TARGETS_OF_RUNX1_RUNX1T1_FUSION_MONOCYTE_DN	0
RICKMAN_TUMOR_DIFFERENTIATED_WELL_VS_POORLY_DN	0
KEGG_ARRHYTHMOGENIC_RIGHT_VENTRICULAR_CARDIOMYOPAT	0
PID_GMCSF_PATHWAY	0
PID_EPHB_FWD_PATHWAY	0
REACTOME_REGULATION_OF_LIPID_METABOLISM_BY_PEROXISO	0
HAN_JNK_SINGALING_DN	0
REACTOME_SEMAPHORIN_INTERACTIONS	0
KYNG_NORMAL_AGING_DN	0
BIOCARTA_NUCLEARRS_PATHWAY	0
TAKEDA_TARGETS_OF_NUP98_HOXA9_FUSION_8D_DN	0
PID_IL4_2PATHWAY	0
WANG_RESPONSE_TO_GSK3_INHIBITOR_SB216763_UP	0
PID_IL6_7_PATHWAY	0
LUI_THYROID_CANCER_CLUSTER_2	0
FLECHNER_BIOPSY_KIDNEY_TRANSPLANT_REJECTED_VS_OK_UP	0
ZHAN_MULTIPLE_MYELOMA_CD1_VS_CD2_UP	0
RODWELL_AGING_KIDNEY_NO_BLOOD_UP	0
ZHAN_MULTIPLE_MYELOMA_CD1_DN	0
DIAZ_CHRONIC_MEYLOGENOUS_LEUKEMIA_DN	0
MARTIN_NFKB_TARGETS_UP	0
JECHLINGER_EPITHELIAL_TO_MESENCHYMAL_TRANSITION_DN	0
SCHOEN_NFKB_SIGNALING	0
PETROVA_PROX1_TARGETS_DN	0
KEGG_ALLOGRAFT_REJECTION	0
LU_TUMOR_ENDOTHELIAL_MARKERS_UP	0
TAKEDA_TARGETS_OF_NUP98_HOXA9_FUSION_10D_DN	0
YAO_HOXA10_TARGETS_VIA_PROGESTERONE_UP	0
HOFFMANN_LARGE_TO_SMALL_PRE_BII_LYMPHOCYTE_DN	0
NIKOLSKY_BREAST_CANCER_17Q21_Q25_AMPLICON	0
HOEBEKE_LYMPHOID_STEM_CELL_UP	0
MARTIN_VIRAL_GPCR_SIGNALING_UP	0
ZHANG_BREAST_CANCER_PROGENITORS_DN	0
REACTOME_HEPARAN_SULFATE_HEPARIN_HS_GAG_METABOLISM	0
WANG_ESOPHAGUS_CANCER_VS_NORMAL_UP	0

PID_PTP1B_PATHWAY	0
REACTOME_TRANSCRIPTIONAL_REGULATION_BY_THE_AP_2_TFA	0
VERHAAK_AML_WITH_NPM1_MUTATED_UP	0
TAVOR_CEBPA_TARGETS_UP	0
PID_NECTIN_PATHWAY	0
YANG_BREAST_CANCER_ESR1_BULK_DN	0
KEGG_CELL_ADHESION_MOLECULES_CAMS	0
KOBAYASHI_EGFR_SIGNALING_24HR_UP	0
FAELT_B_CLL_WITH_VH_REARRANGEMENTS_UP	0
HORIUCHI_WTAP_TARGETS_UP	0
REACTOME_IMMUNOREGULATORY_INTERACTIONS_BETWEEN_A	0
REACTOME_INTERACTION_BETWEEN_L1_AND_ANKYRINS	0
REACTOME_PHOSPHOLIPID_METABOLISM	0
MATSUDA_NATURAL_KILLER_DIFFERENTIATION	0
CROONQUIST_NRAS_VS_STROMAL_STIMULATION_UP	0
WIELAND_UP_BY_HBV_INFECTION	0
VERHAAK_GLIOBLASTOMA_MESENCHYMAL	0
BIOCARTA_NKT_PATHWAY	0
BOYLAN_MULTIPLE_MYELOMA_C_DN	0
SAKAI_TUMOR_INFILTRATING_MONOCYTES_UP	0
MAHAJAN_RESPONSE_TO_IL1A_DN	0
BANDRES_RESPONSE_TO_CARMUSTIN_MGMT_24HR_DN	0
MARZEC_IL2_SIGNALING_DN	0
BORCZUK_MALIGNANT_MESOTHELIOMA_DN	0
CHO_NR4A1_TARGETS	0
CASORELLI_ACUTE_PROMYELOCYTIC_LEUKEMIA_UP	0
BIOCARTA_IL1R_PATHWAY	0
BIOCARTA_TOLL_PATHWAY	0
WORSCHECH_TUMOR_REJECTION_UP	0
BIOCARTA_LAIR_PATHWAY	0
PID_RB_1PATHWAY	0
PID_SYNDECAN_3_PATHWAY	0
BURTON_ADIPOGENESIS_8	0
PID_TCPTP_PATHWAY	0
PEREZ_TP53_AND_TP63_TARGETS	0
BROWNE_HCMV_INFECTION_18HR_DN	0
REACTOME_GLYCEROPHOSPHOLIPID_BIOSYNTHESIS	0
PARK_APL_PATHOGENESIS_DN	0
PID_DELTA_NP63_PATHWAY	0
MORI_PLASMA_CELL_DN	0
HESS_TARGETS_OF_HOXA9_AND_MEIS1_DN	0
YAO_TEMPORAL_RESPONSE_TO_PROGESTERONE_CLUSTER_0	0
LIAN_NEUTROPHIL_GRANULE_CONSTITUENTS	0
CASORELLI_APL_SECONDARY_VS_DE_NOVO_UP	0
HAHTOLA_MYCOSIS_FUNGOIDES_CD4_UP	0

SMID_BREAST_CANCER_NORMAL_LIKE_UP	0
CROONQUIST_NRAS_SIGNALING_UP	0
SEKI_INFLAMMATORY_RESPONSE_LPS_UP	0
KEGG_DILATED_CARDIOMYOPATHY	0
REACTOME_SIGNALING_BY_RETINOIC_ACID	0
THEODOROU_MAMMARY_TUMORIGENESIS	0
HERNANDEZ_ABERRANT_MITOSIS_BY_DOCETACEL_4NM_UP	0
MORI_LARGE_PRE_BII_LYMPHOCYTE_DN	0
PEREZ_TP63_TARGETS	0
GAVIN_FOXP3_TARGETS_CLUSTER_P3	0
ROZANOV_MMP14_TARGETS_DN	0
PID_EPO_PATHWAY	0
HOWLIN_PUBERTAL_MAMMARY_GLAND	0
YU_MYC_TARGETS_DN	0
CLIMENT_BREAST_CANCER_COPY_NUMBER_UP	0
GRAESSMANN_RESPONSE_TO_MC_AND_SERUM_DEPRIVATION_I	0
KEGG_AXON_GUIDANCE	0
NABA_ECM_AFFILIATED	0
KEGG_PROSTATE_CANCER	0
GAURNIER_PSMD4_TARGETS	0
CHEN_LVAD_SUPPORT_OF_FAILING_HEART_UP	0
RODRIGUES_NTN1_TARGETS_DN	0
STEGER_ADIPOGENESIS_UP	0
VERNOCHET_ADIPOGENESIS	0
BIOCARTA_SPPA_PATHWAY	0
BROWNE_HCMV_INFECTION_30MIN_UP	0
PID_ATF2_PATHWAY	0
RODWELL_AGING_KIDNEY_UP	0
SMIRNOV_RESPONSE_TO_IR_6HR_UP	0
REACTOME_DEFECTIVE_B4GALT7_CAUSES_EDS_PROGEROID_TYPI	0
SHIN_B_CELL_LYMPHOMA_CLUSTER_8	0
OLSSON_E2F3_TARGETS_UP	0
MOROSETTI_FACIOSCAPULOHUMERAL_MUSCULAR_DISTROPHY_U	0
RAY_TUMORIGENESIS_BY_ERBB2_CDC25A_DN	0
BILBAN_B_CLL_LPL_UP	0
ZHAN_MULTIPLE_MYELOMA_LB_UP	0
KEGG_HYPERTROPHIC_CARDIOMYOPATHY_HCM	0
PID_CMYB_PATHWAY	0
POOLA_INVASIVE_BREAST_CANCER_DN	0
HELLER_SILENCED_BY_METHYLATION_UP	0
ONO_FOXP3_TARGETS_UP	0
RODRIGUES_DCC_TARGETS_DN	0
PID_NCADHERIN_PATHWAY	0
BOSCO_TH1_CYTOTOXIC_MODULE	0
COATES_MACROPHAGE_M1_VS_M2_DN	0

LU_TUMOR_VASCULATURE_UP	0
YAUCH_HEDGEHOG_SIGNALING_PARACRINE_UP	0
KONDO_PROSTATE_CANCER_WITH_H3K27ME3	0
KEGG_MELANOMA	0
REACTOME_ROS_AND_RNS_PRODUCTION_IN_PHAGOCYTES	0
BONOME_OVARIAN_CANCER_SURVIVAL_OPTIMAL_DEBULKING	0
VALK_AML_CLUSTER_9	0
REACTOME_CIRCADIAN_CLOCK	0
RUTELLA_RESPONSE_TO_HGF_DN	0
SCHLESINGER_H3K27ME3_IN_NORMAL_AND_METHYLATED_IN_CA	0
MASSARWEH_TAMOXIFEN_RESISTANCE_DN	0
KLEIN_PRIMARY_EFFUSION_LYMPHOMA_DN	0
KEGG_CYTOKINE_CYTOKINE_RECEPTOR_INTERACTION	0
FOSTER_TOLERANT_MACROPHAGE_UP	0
SHEN_SMARCA2_TARGETS_DN	0
KEGG_REGULATION_OF_ACTIN_CYTOSKELETON	0
AMIT_SERUM_RESPONSE_40_MCF10A	0
REACTOME_COMPLEMENT_CASCADE	0
WALLACE_PROSTATE_CANCER_RACE_UP	0
ALTEMEIER_RESPONSE_TO_LPS_WITH_MECHANICAL_VENTILATIO	0
NOUZOVA_METHYLATED_IN_APL	0
REACTOME_NEUTROPHIL_DEGRANULATION	0
KUROZUMI_RESPONSE_TO_ONCOCYTIC_VIRUS	0
CHARAFE_BREAST_CANCER_LUMINAL_VS_MESENCHYMAL_UP	0
KEGG_PATHWAYS_IN_CANCER	0
SHETH_LIVER_CANCER_VS_TXNIP_LOSS_PAM5	0
MOLENAAR_TARGETS_OF_CCND1_AND_CDK4_UP	0
FOSTER_TOLERANT_MACROPHAGE_DN	0
WANG_TNF_TARGETS	0
BIOCARTA_ETS_PATHWAY	0
GAVIN_FOXP3_TARGETS_CLUSTER_P4	0
WANG_IMMORTALIZED_BY_HOXA9_AND_MEIS1_UP	0
REACTOME_CLATHRIN_MEDIATED_ENDOCYTOSIS	0
MOREAUX_MULTIPLE_MYELOMA_BY_TACI_UP	0
ZHU_SKIL_TARGETS_UP	0
KOYAMA_SEMA3B_TARGETS_UP	0
CARD_MIR302A_TARGETS	0
PHONG_TNF_RESPONSE_VIA_P38_PARTIAL	0
IKEDA_MIR30_TARGETS_DN	0
BASSO_CD40_SIGNALING_DN	0
REACTOME_TNFS_BIND_THEIR_PHYSIOLOGICAL_RECEPTORS	0
ROSS_AML_WITH_MLL_FUSIONS	0
KANG_IMMORTALIZED_BY_TERT_UP	0
ALONSO_METASTASIS_NEURAL_UP	0
KEGG_CHEMOKINE_SIGNALING_PATHWAY	0

HELLEBREKERS_SILENCED_DURING_TUMOR_ANGIOGENESIS	0
KYNG_DNA_DAMAGE_BY_4NQO_OR_UV	0
GAUSSMANN_MLL_AF4_FUSION_TARGETS_F_UP	0
URS_ADIPOCYTE_DIFFERENTIATION_UP	0
REACTOME_SIGNALING_BY_ERBB4	0
MARTIN_INTERACT_WITH_HDAC	0
DUTERTRE_ESTRADIOL_RESPONSE_6HR_DN	0
CHYLA_CBFA2T3_TARGETS_UP	0
PURBEY_TARGETS_OF_CTBP1_NOT_SATB1_DN	0
BOSCO_ALLERGEN_INDUCED_TH2_ASSOCIATED_MODULE	0
FIRESTEIN_PROLIFERATION	0
DURAND_STROMA_S_UP	0
GAZDA_DIAMOND_BLACKFAN_ANEMIA_ERYTHROID_DN	0
KESHELAVA_MULTIPLE_DRUG_RESISTANCE	0
BHAT_ESR1_TARGETS_NOT_VIA_AKT1_DN	0
HOLLERN_EMT_BREAST_TUMOR_DN	0
APPIERTO_RESPONSE_TO_FENRETINIDE_UP	0
REACTOME_SYNTHESIS_OF_IP3_AND_IP4_IN_THE_CYTOSOL	0
PID_SHP2_PATHWAY	0
MASSARWEH_TAMOXIFEN_RESISTANCE_UP	0
RIGGI_EWING_SARCOMA_PROGENITOR_UP	0
LIN_TUMOR_ESCAPE_FROM_IMMUNE_ATTACK	0
LIM_MAMMARY_LUMINAL_MATURE_UP	0
OSADA_ASCL1_TARGETS_UP	0
TURASHVILI_BREAST_CARCINOMA_DUCTAL_VS_LOBULAR_UP	0
ZHANG_RESPONSE_TO_IKK_INHIBITOR_AND_TNF_UP	0
XU_GH1_AUTOCRINE_TARGETS_UP	0
REACTOME_OTHER_INTERLEUKIN_SIGNALING	0
CUI_TCF21_TARGETS_DN	0
GRAHAM_CML_QUIESCENT_VS_NORMAL_DIVIDING_UP	0
DURCHDEWALD_SKIN_CARCINOGENESIS_DN	0
BIOCARTA_FMLP_PATHWAY	0
ACEVEDO_LIVER_TUMOR_VS_NORMAL_ADJACENT_TISSUE_DN	0
TARTE_PLASMA_CELL_VS_PLASMABLAST_UP	0
ASTON_MAJOR_DEPRESSIVE_DISORDER_DN	0
RUTELLA_RESPONSE_TO_HGF_VS_CSF2RB_AND_IL4_DN	0
VILIMAS_NOTCH1_TARGETS_DN	0
BROWNE_HCMV_INFECTION_20HR_UP	0
REACTOME_NETRIN_1_SIGNALING	0
REACTOME_PI3K_AKT_SIGNALING_IN_CANCER	0
BHAT_ESR1_TARGETS_VIA_AKT1_DN	0
REACTOME_INTERLEUKIN_10_SIGNALING	0
ZHOU_INFLAMMATORY_RESPONSE_FIMA_UP	0
AFFAR_YY1_TARGETS_UP	0
ODONNELL_TFRC_TARGETS_UP	0

NABA_MATRISOME_ASSOCIATED	0
DUAN_PRDM5_TARGETS	0
MIKKELSEN_NPC_HCP_WITH_H3K4ME3_AND_H3K27ME3	0
LINDGREN_BLADDER_CANCER_CLUSTER_1_UP	0
BOYLAN_MULTIPLE_MYELOMA_C_CLUSTER_DN	0
KEGG_SPHINGOLIPID_METABOLISM	0
MCCABE_BOUND_BY_HOXC6	0
PHONG_TNF_RESPONSE_VIA_P38_COMPLETE	0
PEDRIOLI_MIR31_TARGETS_UP	0
KEGG_INSULIN_SIGNALING_PATHWAY	0
REACTOME_G_ALPHA_I_SIGNALLING_EVENTS	0
DAVIES_MULTIPLE_MYELOMA_VS_MGUS_DN	0.00376648
HAHTOLA_SEZARY_SYNDROM_DN	0.00409836
CHEMNITZ_RESPONSE_TO_PROSTAGLANDIN_E2_DN	0.00424628
BOQUEST_STEM_CELL_UP	0.00434783
BERENJENO_TRANSFORMED_BY_RHOA_FOREVER_DN	0.00796813
KEGG_ETHER_LIPID_METABOLISM	0.00914077
ZHOU_INFLAMMATORY_RESPONSE_LIVE_UP	0.0092081
SHIN_B_CELL_LYMPHOMA_CLUSTER_7	0.00938086
HOFMANN_MYELODYSPLASTIC_SYNDROM_RISK_DN	0.0093985
YAGI_AML_RELAPSE_PROGNOSIS	0.0095057
MCCLUNG_CREB1_TARGETS_DN	0.00952381
PID_TXA2PATHWAY	0.00968992
PID_RXR_VDR_PATHWAY	0.00970874
ZIRN_TRETINOIN_RESPONSE_WT1_UP	0.00974659
WANG_METASTASIS_OF_BREAST_CANCER_ESR1_DN	0.00982318
SWEET_LUNG_CANCER_KRAS_UP	0.00982318

Supplementary Table 2. Gene Set Enrichment Analyses (GSEA) in PE conditional knockout leukemias. GSEA analyses against the C2 database using our PE conditional knockout T-ALL RNA-seq data revealed 342 gene sets significantly downregulated (nominal $P < 0.01$) upon loss of PE.

Technique	Name	Sequence (5'→ 3')
4C-seq	Human *PTEN* promoter viewpoint (forward)	AAATATCAACACTGAAGCTT
	Human *PTEN* promoter viewpoint (reverse)	GCCTCCAGTTGATTTCCAGA
	Human PE viewpoint (forward)	CAGCTTCTCCTTTTAAGCTT
	Human PE viewpoint (reverse)	CACAGACATAATGCTGGGAA
	Mouse *Pten* promoter viewpoint (forward)	GTTCATCCTGAGTAAAGCTT
	Mouse *Pten* promoter viewpoint (reverse)	CAAAAGATAATTGGTGAGCA
	Mouse PE viewpoint (forward)	CCTCTATATGAGAGAAGCTT
	Mouse PE viewpoint (reverse)	AAGAGCTGGCCACATGGTGA
CRISPR/Cas9	Human PE sgRNA 1 (forward)	GGATCACTTTCCCACTACGA
	Human PE sgRNA 2 (forward)	GGTGGCCCATTATTAACCTG
	Mouse PE sgRNA 1 (forward)	GCCGTTCTTCCTAATGTGCA
	Mouse PE sgRNA 2 (forward)	GGAAGTGTCAACATCACCAG
Genotyping	Human PE CRISPR/Cas9 (forward 1)	GTTGGTAAACTACCATCCATGGGC
	Human PE CRISPR/Cas9 (reverse 1)	TAAGATGTCACAGTACAACGTGGC
	Human PE CRISPR/Cas9 (forward 2)	TGGATGATCCAGGTTAAGCTCTCC
	Human PE CRISPR/Cas9 (reverse 2)	GTGACTAGACCAGAGAATCTGAGG
	Mouse PE CRISPR/Cas9 (forward 1)	CACTGAGCACTCAAGATGCAAGC
	Mouse PE CRISPR/Cas9 (reverse 1)	GGTCCTTCTGAAGACAGTGTCAG
	Mouse PE CRISPR/Cas9 (forward 2)	CTCATATAGAGGAAGAGCTGGCC
	Mouse PE CRISPR/Cas9 g (reverse 2)	TGCAGGATACCTGATACACGAGC
	Mouse PE Flox (loxP1 forward)	CAGCGATATGGCATAAGCACCTG
	Mouse PE Flox (loxP1 reverse)	ACCAGCAGCCACATCAGCTACAG
	Mouse PE Flox (loxP2 forward 2)	GAAAGACTCTGAACTTCCATGTCTC
	Mouse PE Flox (loxP2 reverse 2)	GATAATGCAGGATACCTGATACACG
qRT-PCR	Human *PTEN* (forward)	AGCGTGCAGATAATGACAAGG
	Human *PTEN* (reverse)	TGGATCAGAGTCAGTGGTGTC
	Mouse *Pten* (forward)	GGGGAAGTAAGGACCAGAGACAAA
	Mouse *Pten* (reverse)	CCACGGGTCTGTAATCCAGGTG
	Human *RNLS* (forward)	GTCCGGTCCCTTGTACCTTG
	Human *RNLS* (reverse)	TGCAGGTGATGTACTGAGCAC
	Mouse *Rnls* (forward)	AAATCTGTGAGCTACTCCTCTCG
	Mouse *Rnls* (reverse)	CAGGACCAAGGGACACCAA
	Mouse *β-Actin* (forward)	GGCTGTATTCCCCTCCATCG
	Mouse *β-Actin* (reverse)	CCAGTTGGTAACAATGCCATGT
	Human *GAPDH* (forward)	GAAGGTGAAGGTCGGAGT
	Human *GAPDH* (reverse)	GAAGATGGTGATGGGATTTC
	Mouse *Gapdh* (forward)	TGGCAAAGTGGAGATTGTTGCC
	Mouse *Gapdh* (reverse)	AAGATGGTGATGGGCTTCCCG

Supplementary Table 3. Oligonucleotide sequences.

Technique	Target	Company	Clone	Cat. number	Dilution	Lot. Number
IHC	PTEN	Cell Signaling	D4.3	9188	1:200	6, 11/2019
ChIPmentation	H3K27ac	Diagenode	Polyclonal	C15410174	2.33µg/sample	A1723-0041D
Western Blot	GAPDH	Cell Signaling	D4C6R	97166	1:1000	5, 08/2019
	pAKT(T308)	Cell Signaling	D25E6	13038	1:1000	7, 12/2019
	panAKT	Cell Signaling	11E7	4685	1:1000	6, 10/2017
	PTEN	Cell Signaling	D4.3	9188	1:1000	6, 11/2019
	ACTIN-HRP	Sigma-Aldrich	AC-15	A3854	1:50000	048M4859V
	anti-mouse IgG-HRP	GE Healthcare		NA931V	1:10000	9850216
	anti-rabbit IgG-HRP	GE Healthcare		NA934V	1:10000	
Flow Cytometry	CD8-α PE	BD	53-6.7	553033	1:200	7194728
	CD4 PE-eFluor 610	Thermo Fisher	RM4-5	61-0042-82	1:400	2044771
	CD25 AF488	Thermo Fisher	7D4	53-0252-82	1:1000	4310205
	CD44 PerCP-Cy5.5	Thermo Fisher	IM7	45-0441-82	1:400	4329935
	Ly6A/E (Sca-1) PE	BD	E13-161.7	553336	1:400	7248964
	CD19 PE-Cy7	Thermo Fisher	1D3	25-0193-82	1:1200	4341605
	CD45R PE	Thermo Fisher	RA3-6B2	12-0452-82	1:1000	4339622
	CD8a FITC	Thermo Fisher	53-6.7	11-0081-81	1:200	4329214
	PTEN PE	BD	A2B1	560002	1:400	8219517
	PE Mouse IgG1 k isotype	BD		559320	1:400	9115544
CD4-CD3-enrichment	CD4 Biotin	Thermo Fisher	GK1.5	13-0041-85	1:500	4320100
	CD3ε Biotin	Thermo Fisher	145-2C11	13-0031-85	1:500	2072705
	Streptavidin MicroBeads	Miltenyi Biotec		130-048-101	20µL per 10^7 t cells	5180427037

Supplementary Table 4. Antibodies.